

Supporting information for:

Mechanisms of Neptunium Redox Reactions in Nitric Acid Solutions

Sayandev Chatterjee,* Samuel A Bryan, Amanda J Casella, James M Peterson, and Tatiana G Levitskaia*

Energy and Environment Directorate, Pacific Northwest National Laboratory, Richland, Washington 99352

Determination of diffusion rates for NpO_2^{2+} and NpO_2^+

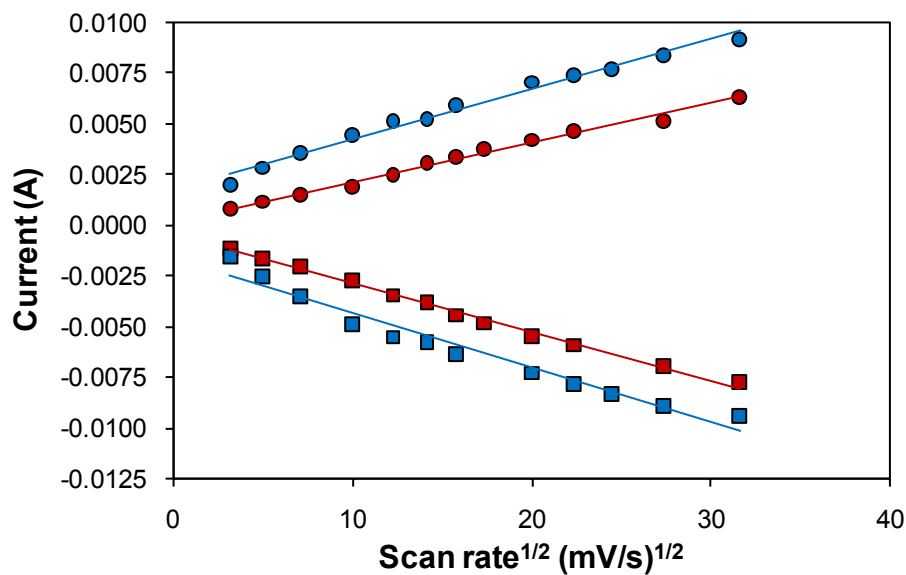


Figure S1. Plot of peak currents versus square root of scan rates: Squares = i_{pa} , Circles = i_{pc} , Red = redox process at ~0.90 V. Blue = redox process at ~-0.10 V.

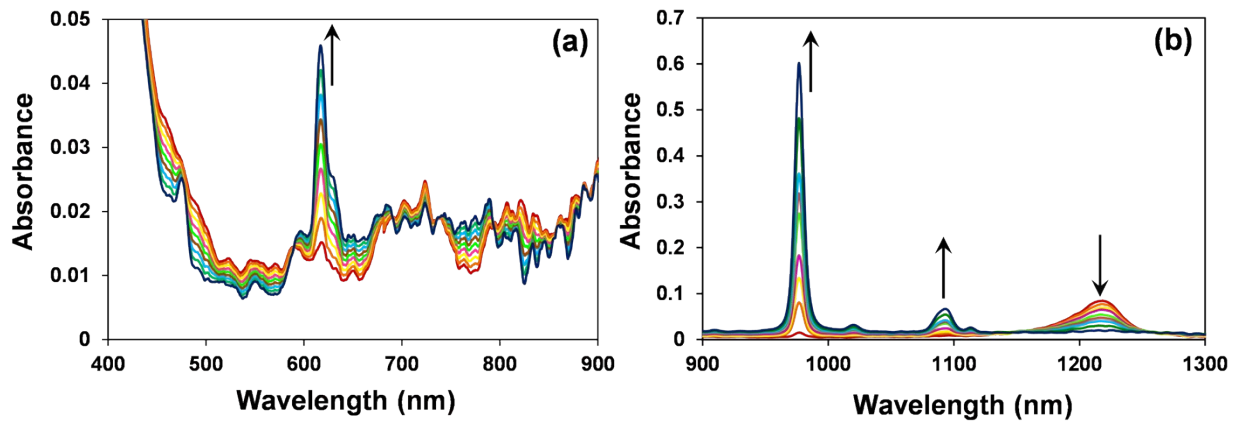


Figure S2. (a) Visible and (b) NIR absorption spectra of 10.3 mM neptunium in 0.50 M HNO₃ recorded between the potentials 1.10 V and 0.60 V as a function of decreasing potentials. The applied potentials are (—) 1.10 V, (—) 1.03 V, (—) 1.01V, (—) 0.99 V, (—) 0.98 V, (—) 0.97 V, (—) 0.95 V, (—) 0.93 V, (—) 0.60 V.

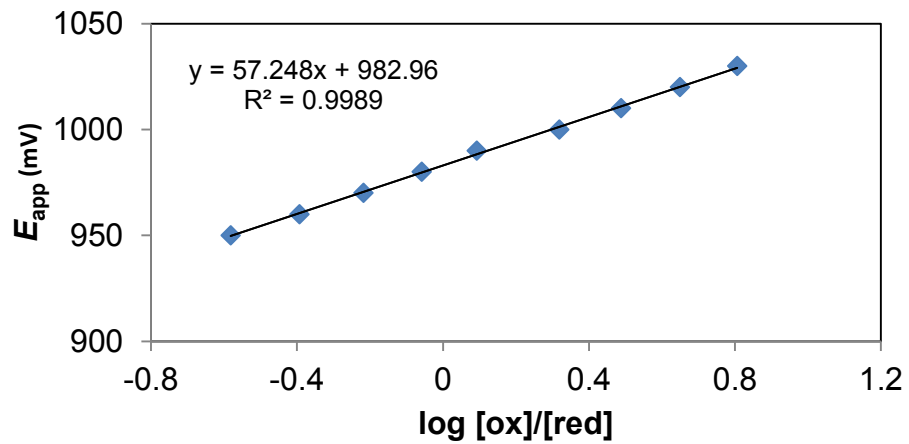


Figure S3. Representative Nernst analysis done at 976 nm for the redox process shown in Figure S1. The corresponding Nernst analysis is: E_{app} (mV) = 982 mV + 57.25 log [ox]/[red]

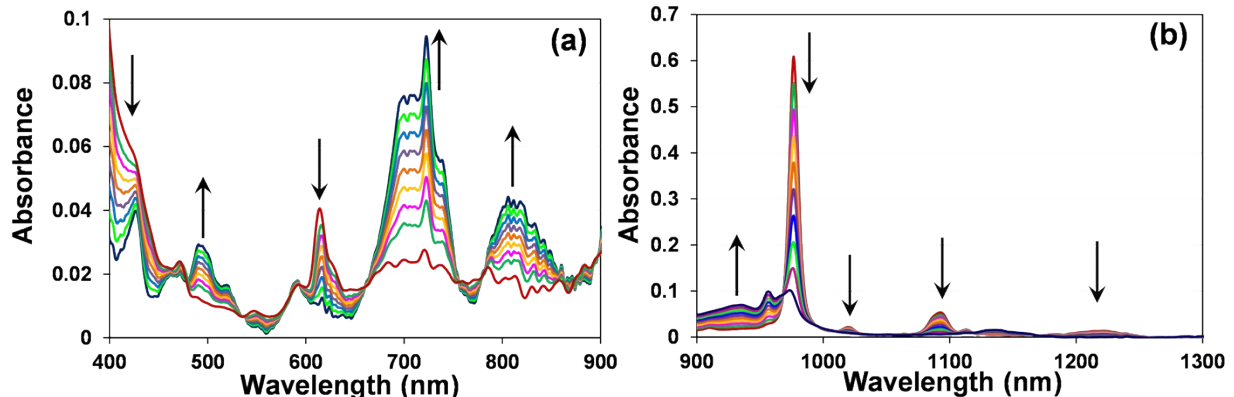


Figure S4. (a) Visible and (b) NIR absorption spectra of 10.3 mM neptunium in 0.5 M HNO₃

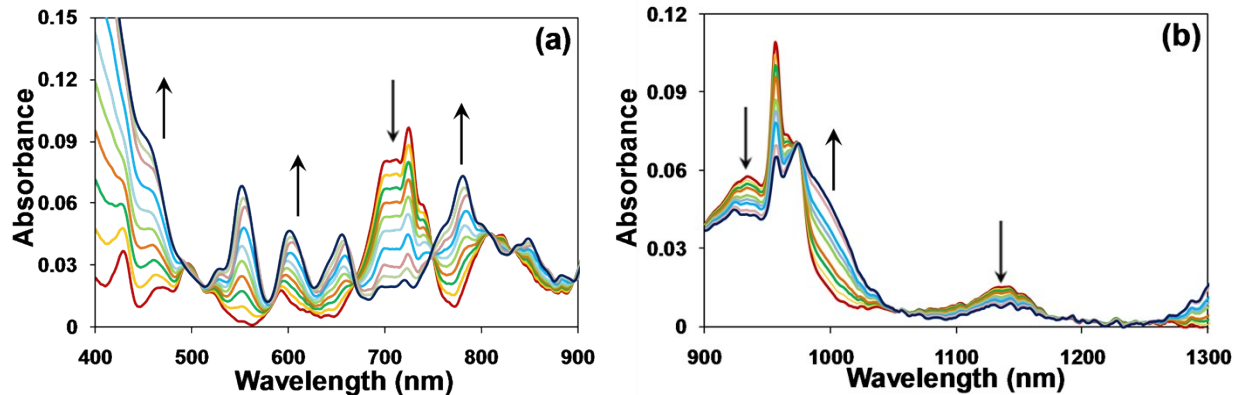


Figure S5. (a) Visible and (b) NIR absorption spectra of 10.3 mM neptunium in 0.50 M HNO₃

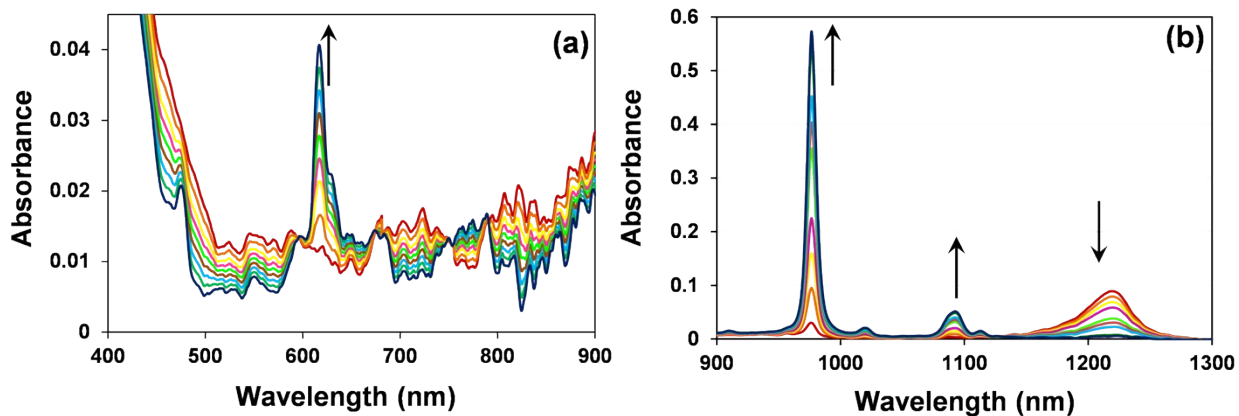


Figure S6. (a) Visible and (b) NIR absorption spectra of 10.3 mM neptunium in 1.28 M HNO₃ recorded between the potentials 1.20 V and 0.30 V as a function of decreasing potentials. The applied potentials are (—) 1.40 V, (—) 1.00 V, (—) 0.99 V, (—) 0.97 V, (—) 0.95 V, (—) 0.92 V, (—) 0.90 V, (—) 0.87 V, (—) 0.80 V.

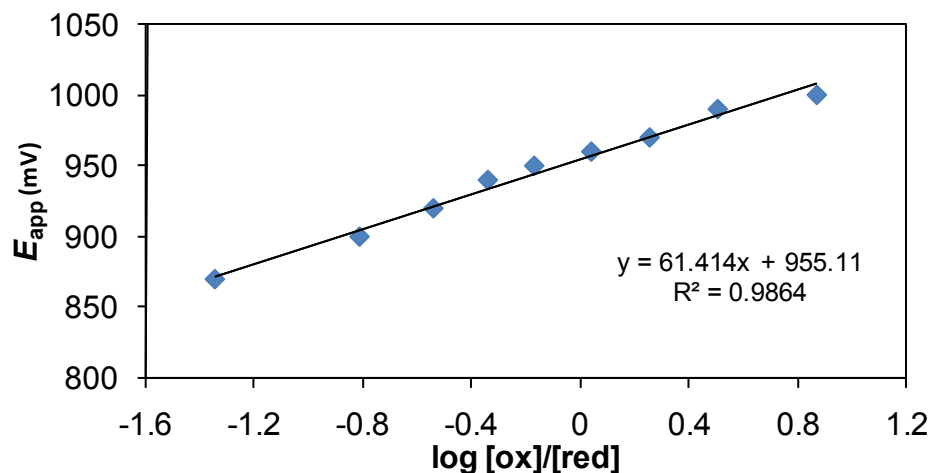


Figure S7. Representative Nernst analysis done at 976 nm for the redox process shown in Figure S1. The corresponding Nernst analysis is: E_{app} (mV) = 955 mV + 61.41 log [ox]/[red]

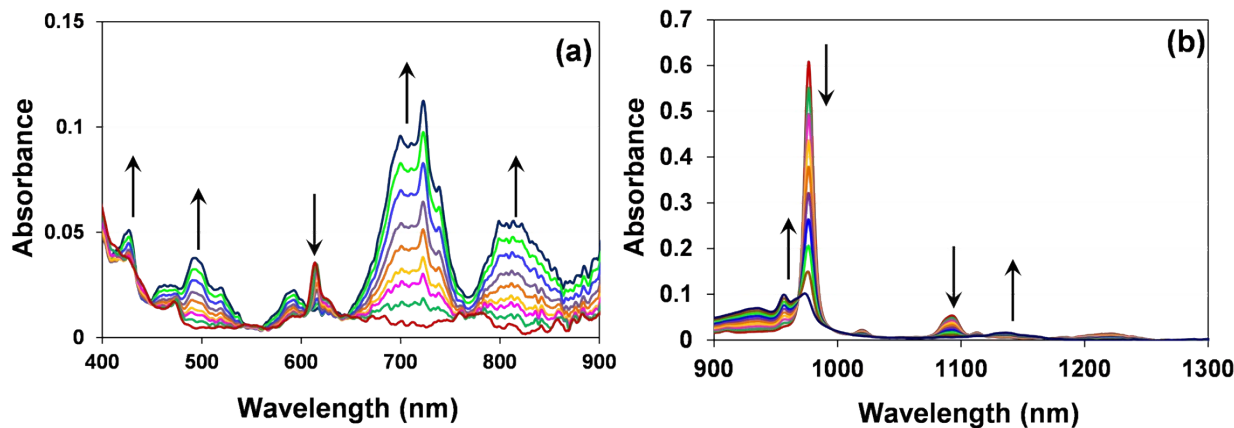


Figure S8. (a) Visible and (b) NIR absorption spectra of 10.3 mM neptunium in 1.28 M HNO₃ recorded between the potentials 0.25 V and 0.05 V as a function of decreasing potentials. The applied potentials are (—) 0.10 V, (—) 0.08 V, (—) 0.06 V, (—) 0.05 V, (—) 0.04 V, (—) 0.03 V, (—) 0.01 V, (—) -0.01 V, (—) -0.03 V, (—) -0.06 V. (The spectrum at -0.03 V was not collected for the UV-visible region)

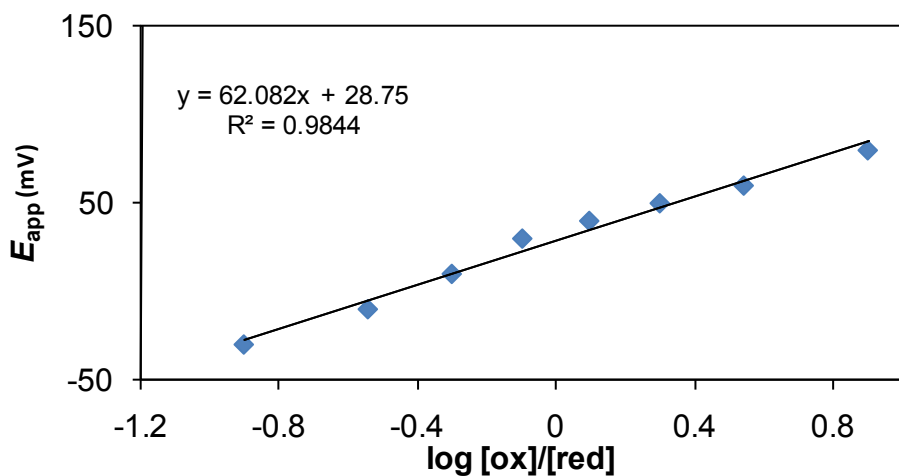


Figure S9. Representative Nernst analysis done at 976 nm for the redox process shown in Figure S8. The corresponding Nernst analysis is: E_{app} (mV) = 29 mV + 62.08 $\log [\text{ox}]/[\text{red}]$

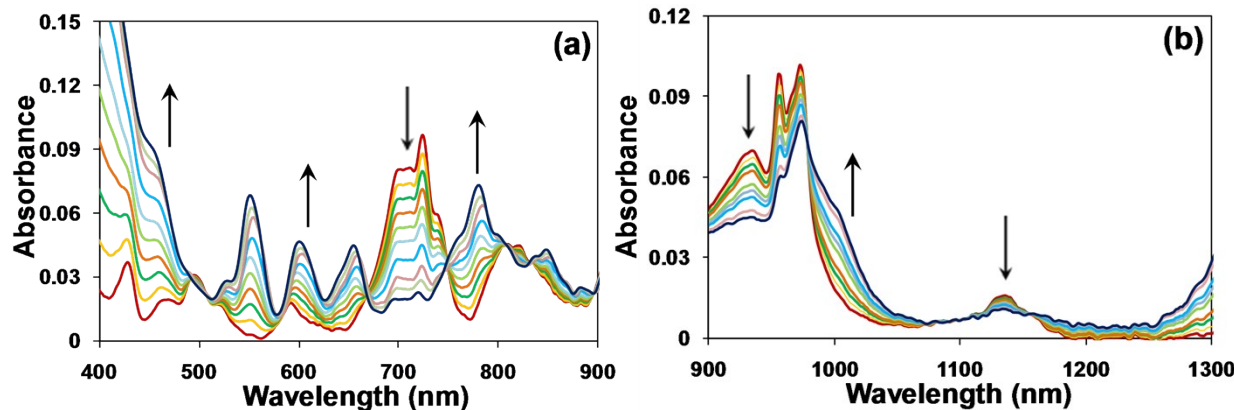


Figure S10. (a) Visible and (b) NIR absorption spectra of 10.3 mM neptunium in 1.28 M HNO₃ recorded between the potentials 0 V and -0.20 V as a function of decreasing potentials. The applied potentials are (—) -0.06 V, (—) -0.07 V, (—) -0.09 V, (—) -0.10 V, (—) -0.11 V, (—) -0.13 V, (—) -0.14 V, (—) -0.15 V, (—) -0.18 V, (—) -0.19 V.

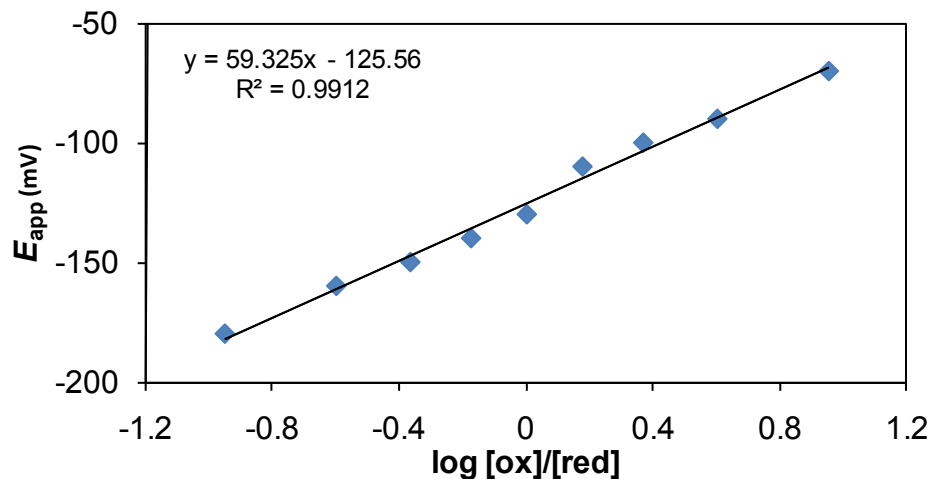


Figure S11. Representative Nernst analysis done at 973 nm for the redox process shown in Figure S10. The corresponding Nernst analysis is: E_{app} (mV) = -126 mV + 59.33 log [ox]/[red]

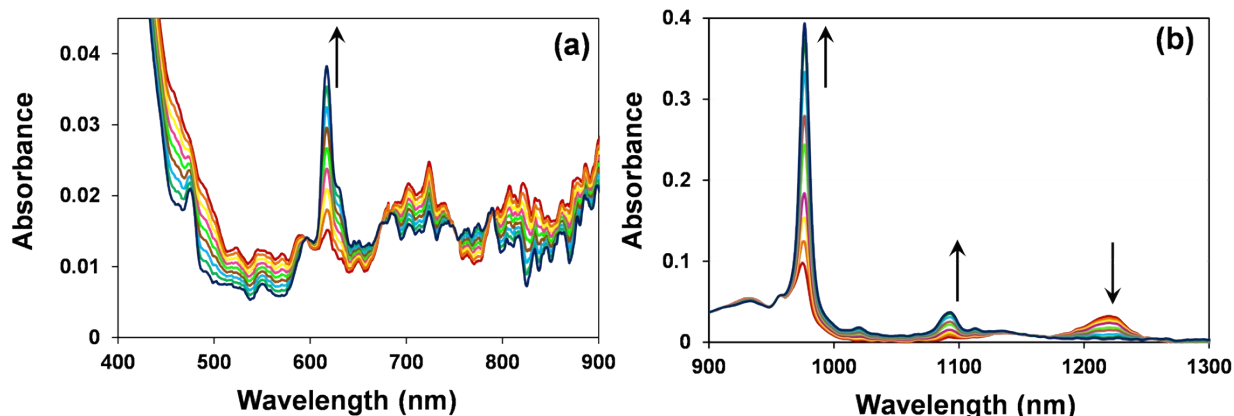


Figure S12. (a) Visible and (b) NIR absorption spectra of 10.3 mM neptunium in 1.55 M HNO₃ recorded between the potentials 1.10 V and 0.60 V as a function of decreasing potentials. The applied potentials are (—) 1.10 V, (—) 0.99 V, (—) 0.97 V, (—) 0.95 V, (—) 0.93 V, (—) 0.91 V, (—) 0.89 V, (—) 0.85 V, (—) 0.60 V.

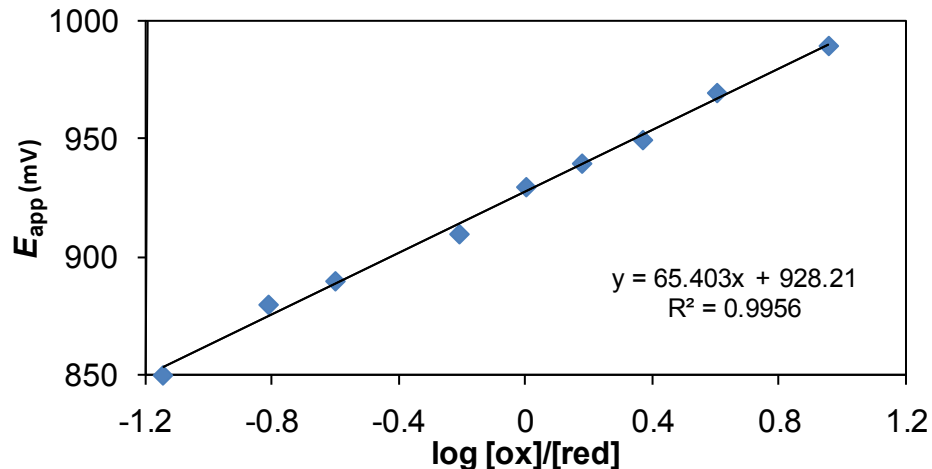


Figure S13. Representative Nernst analysis done at 973 nm for the redox process shown in Figure S12. The corresponding Nernst analysis is: E_{app} (mV) = 928 mV + 65.40 $\log [\text{ox}]/[\text{red}]$

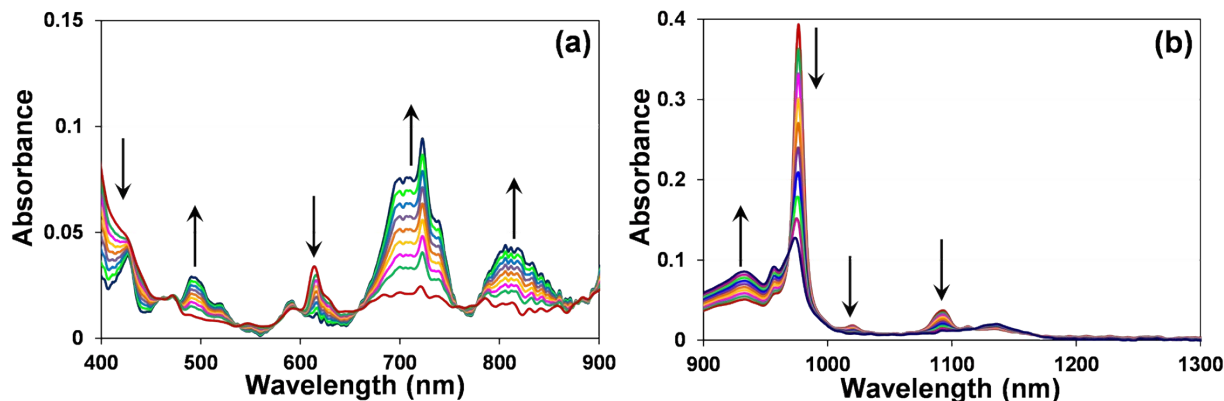


Figure S14. (a) Visible and (b) NIR absorption spectra of 10.3 mM neptunium in 1.55 M HNO₃ recorded between the potentials 0.30 V and -0.05 V as a function of decreasing potentials. The applied potentials are (—) 0.30 V, (—) 0.10 V, (—) 0.08 V, (—) 0.07 V, (—) 0.05 V, (—) 0.04 V, (—) 0.03 V, (—) 0.01 V, (—) 0.00 V, (—) -0.05 V.

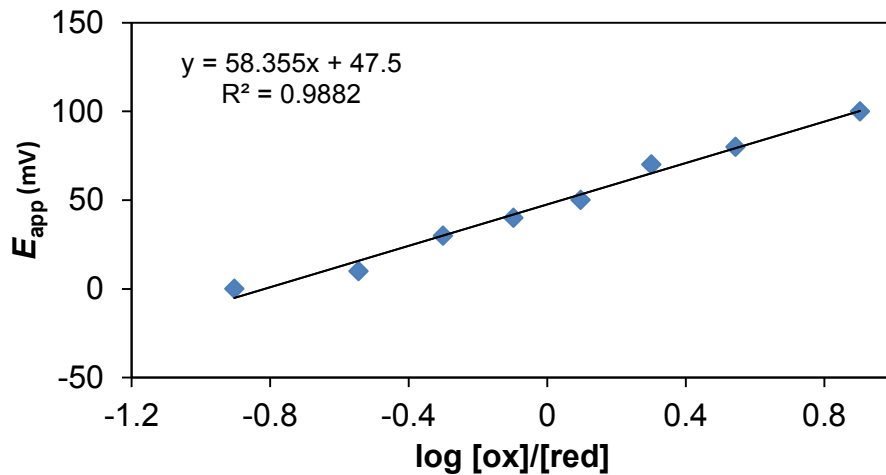


Figure S15. Representative Nernst analysis done at 973 nm for the redox process shown in Figure S14. The corresponding Nernst analysis is: E_{app} (mV) = 47.5 mV + 58.36 log [ox]/[red]

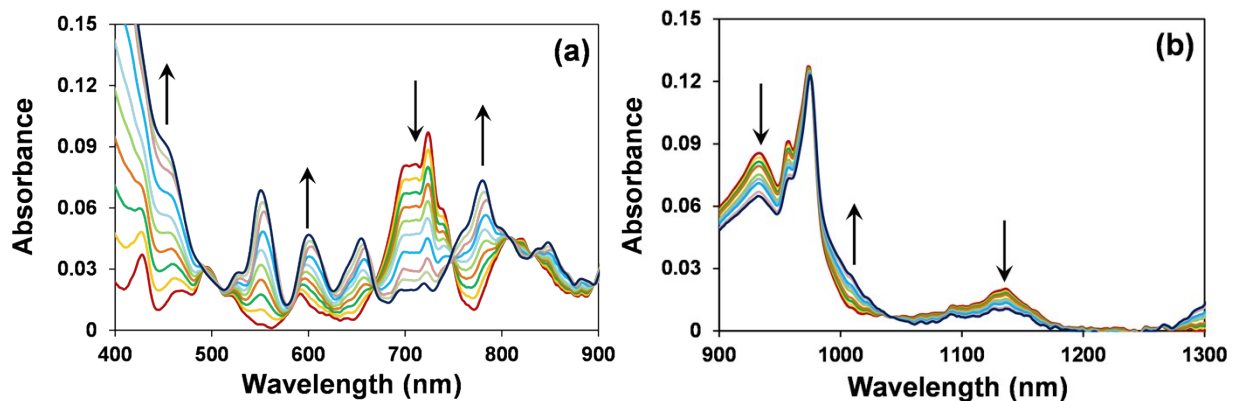


Figure S16. (a) Visible and (b) NIR absorption spectra of 10.3 mM neptunium in 1.55 M HNO₃ recorded between the potentials 0 V and -0.20V as a function of decreasing potentials. The applied potentials are (—) -0.06 V, (—) -0.07 V, (—) -0.09 V, (—) -0.10 V, (—) -0.11 V, (—) -0.13 V, (—) -0.14 V, (—) -0.16 V, (—) -0.18 V, (—) -0.20 V.

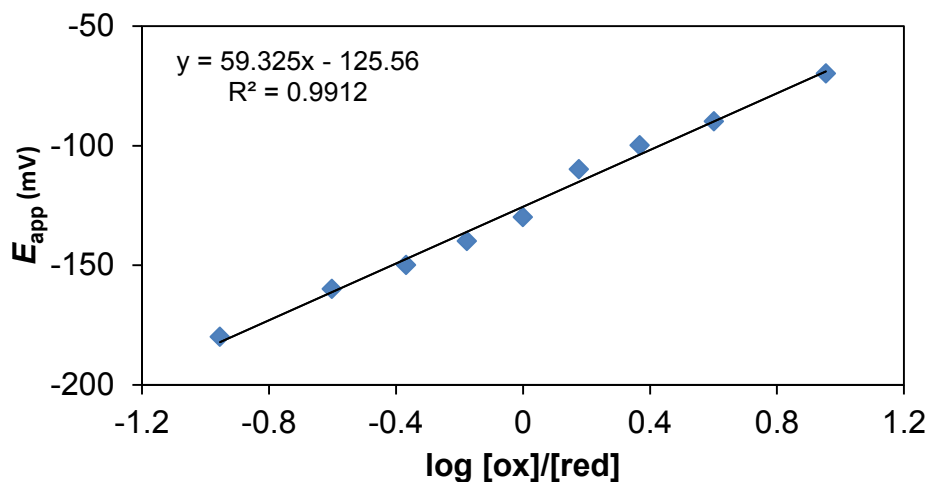


Figure S17. Representative Nernst analysis done at 933 nm for the redox process shown in Figure S16. The corresponding Nernst analysis is: E_{app} (mV) = -125.6 mV + 59.33 log [ox]/[red]

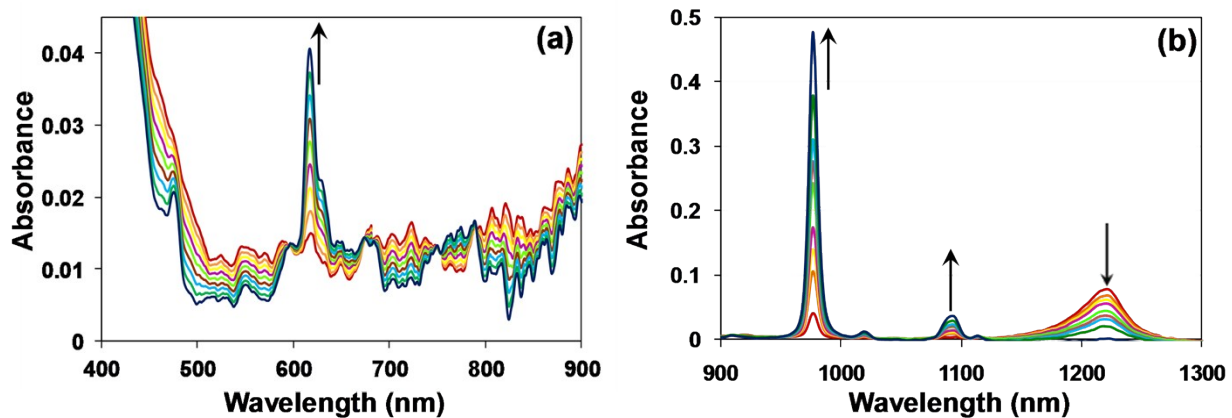


Figure S18. (a) Visible and (b) NIR absorption spectra of 10.3 mM neptunium in 1.79 M HNO₃ recorded between the potentials 1.20 V and 0.30 V as a function of decreasing potentials. The applied potentials are (—) 1.20 V, (—) 0.97 V, (—) 0.96 V, (—) 0.95 V, (—) 0.94 V, (—) 0.93 V, (—) 0.91 V, (—) 0.89 V, (—) 0.80 V.

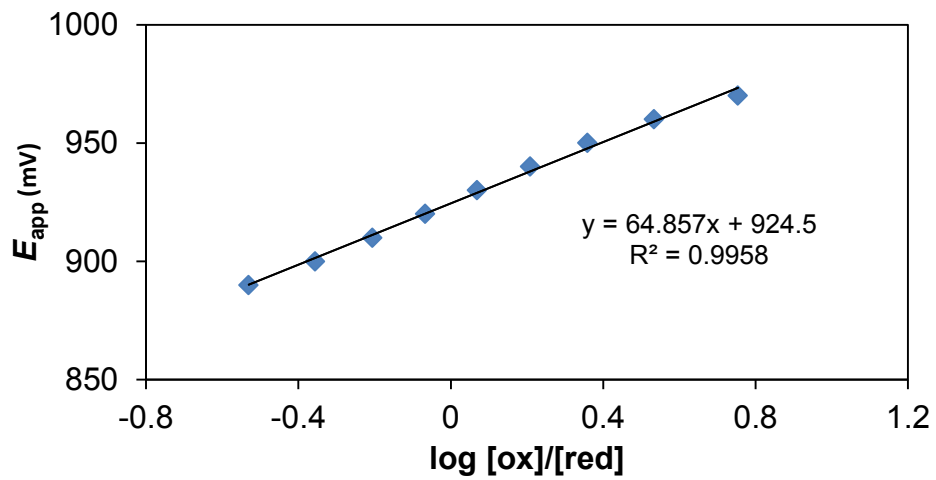


Figure S19. Representative Nernst analysis done at 976 nm for the redox process shown in Figure S18. The corresponding Nernst analysis is: E_{app} (mV) = 925 mV + 64.9 $\log [\text{ox}]/[\text{red}]$

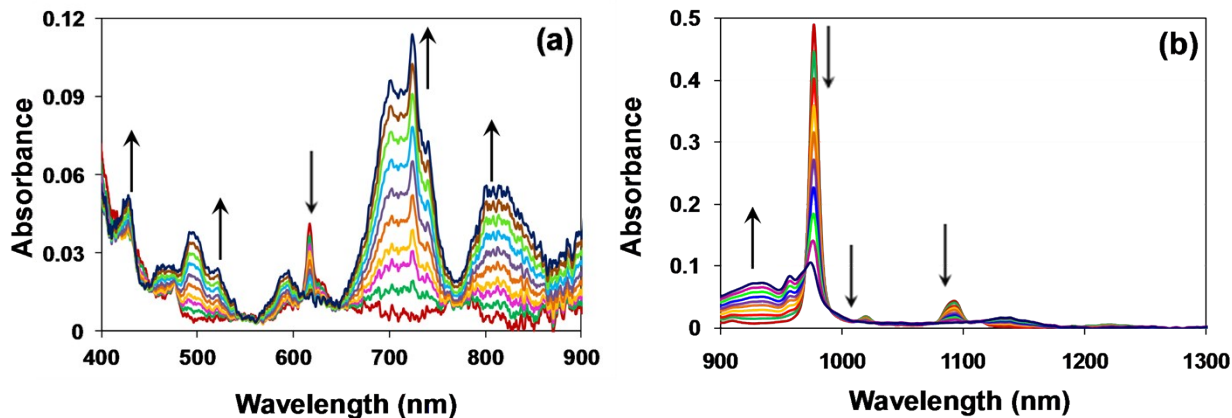


Figure S20. (a) Visible and (b) NIR absorption spectra of 10.3 mM neptunium in 1.79 M HNO₃ recorded between the potentials 0.5 V and -0.05 V as a function of decreasing potentials. The applied potentials are (—) 0.50 V, (—) 0.10 V, (—) 0.08 V, (—) 0.07 V, (—) 0.05 V, (—) 0.04 V, (—) 0.02 V, (—) 0.01 V, (—) 0.0 V, (—) -0.05 V.

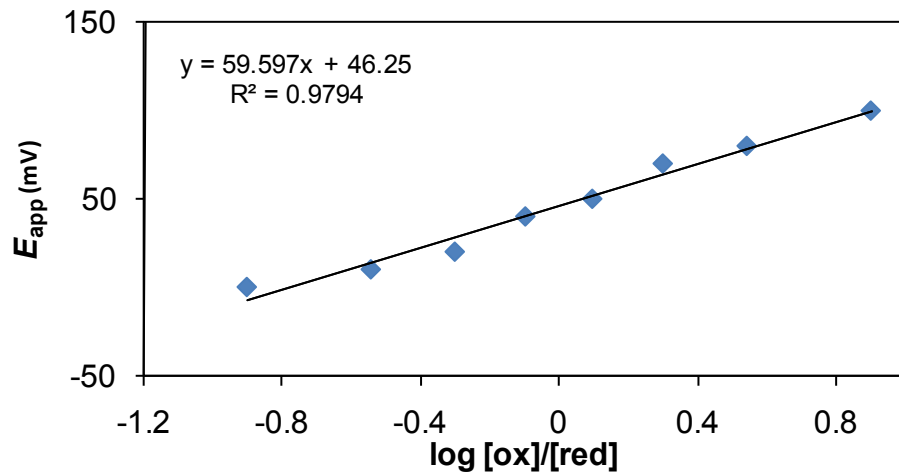


Figure S21. Representative Nernst analysis done at 976 nm for the redox process shown in Figure S20. The corresponding Nernst analysis is: E_{app} (mV) = 46 mV + 59.5 log [ox]/[red]

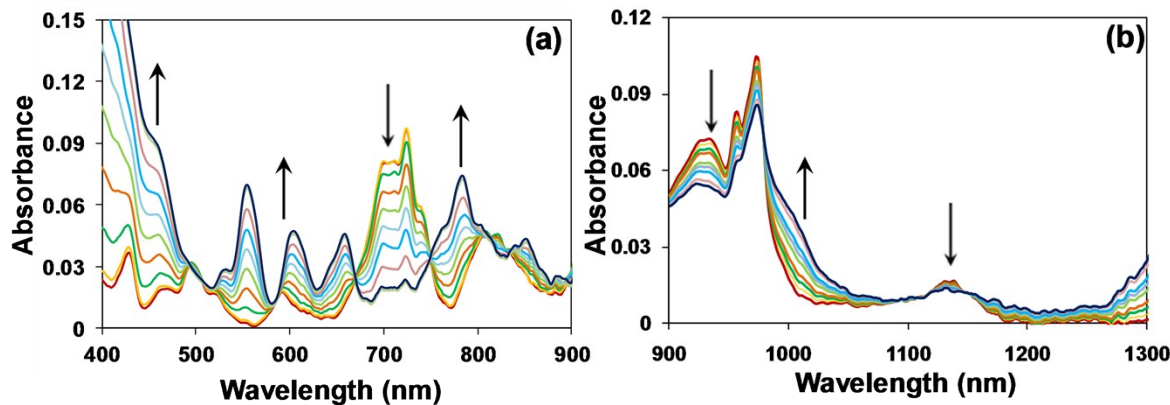


Figure S22. (a) Visible and (b) NIR absorption spectra of 10.3 mM neptunium in 1.79 M HNO₃ recorded between the potentials -0.05 V and -0.20 V as a function of decreasing potentials. The applied potentials are (—) -0.05 V, (—) -0.06 V, (—) -0.07 V, (—) -0.08 V, (—) -0.10 V, (—) -0.11 V, (—) -0.12 V, (—) -0.14 V, (—) -0.16 V, (—) -0.20 V.

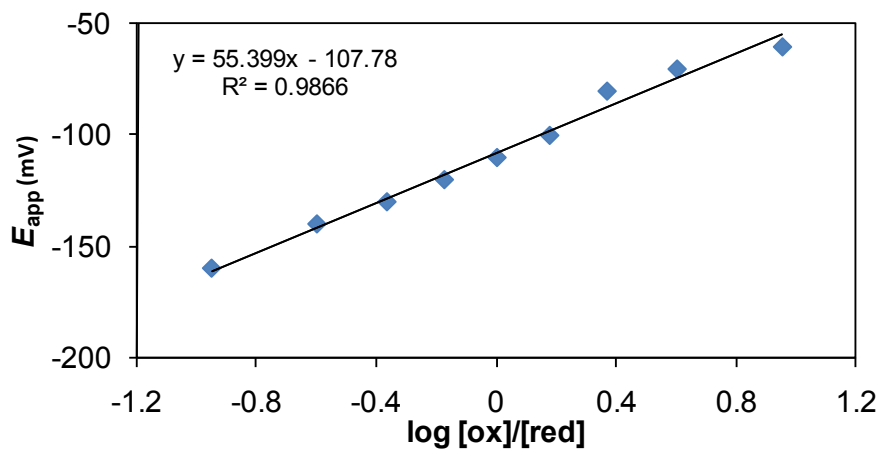


Figure S23. Representative Nernst analysis done at 973 nm for the redox process shown in Figure S22. The corresponding Nernst analysis is: E_{app} (mV) = -108 mV + 55.7 $\log [\text{ox}]/[\text{red}]$

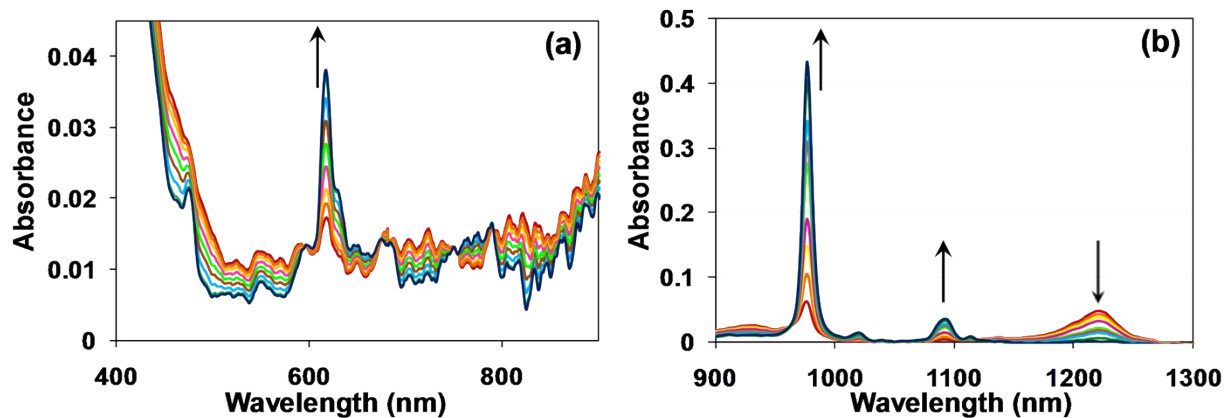


Figure S24. (a) Visible and (b) NIR absorption spectra of 10.3 mM neptunium in 2.92 M HNO_3 recorded between the potentials 1.20 V and 0.30 V as a function of decreasing potentials. The applied potentials are (—) 1.20 V, (—) 1.00 V, (—) 0.99 V, (—) 0.98 V, (—) 0.97 V, (—) 0.96 V, (—) 0.94 V, (—) 0.92 V, (—) 0.80 V.

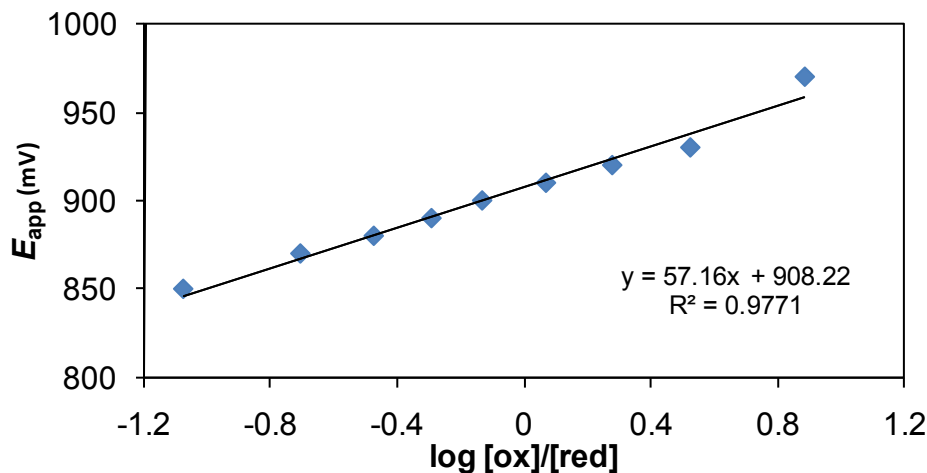


Figure S25. Representative Nernst analysis done at 973 nm for the redox process shown in Figure S24. The corresponding Nernst analysis is: E_{app} (mV) = 908 mV + 57.1 log [ox]/[red]

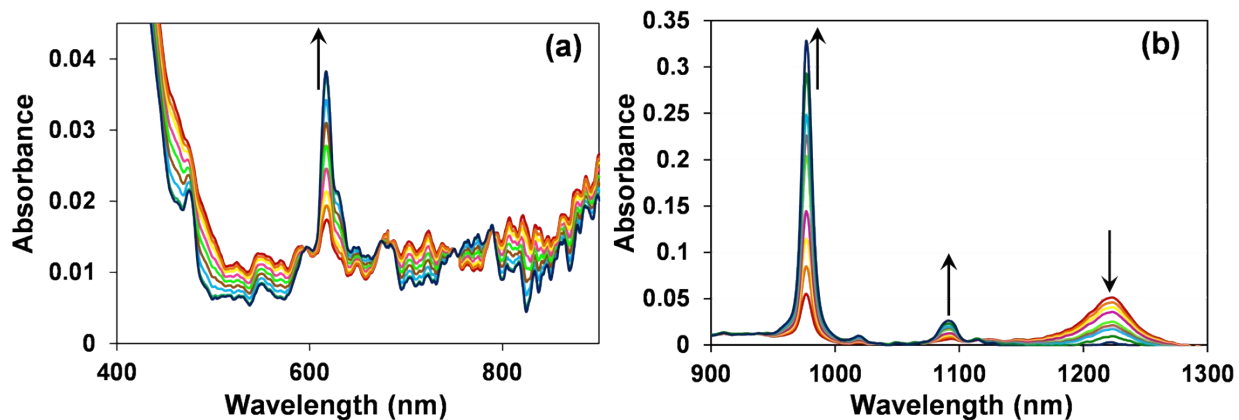


Figure S26. (a) Visible and (b) NIR absorption spectra of 10.3 mM neptunium in 4.00 M HNO₃ recorded between the potentials 1.20 V and 0.30 V as a function of decreasing potentials. The applied potentials are (—) 1.00 V, (—) 0.98 V, (—) 0.96 V, (—) 0.94 V, (—) 0.93 V, (—) 0.91 V, (—) 0.89 V, (—) 0.85 V, (—) 0.82 V.

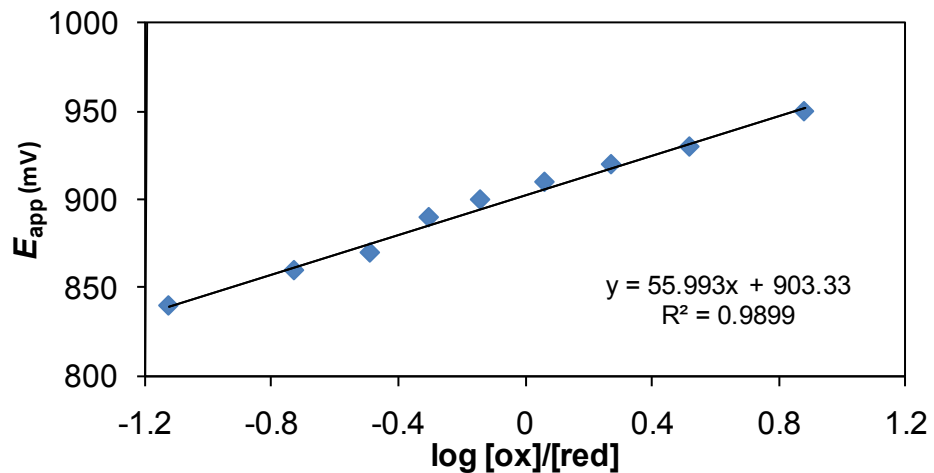


Figure S27. Representative Nernst analysis done at 973 nm for the redox process shown in Figure S26. The corresponding Nernst analysis is: E_{app} (mV) = 903 mV + 56.0 $\log [\text{ox}]/[\text{red}]$

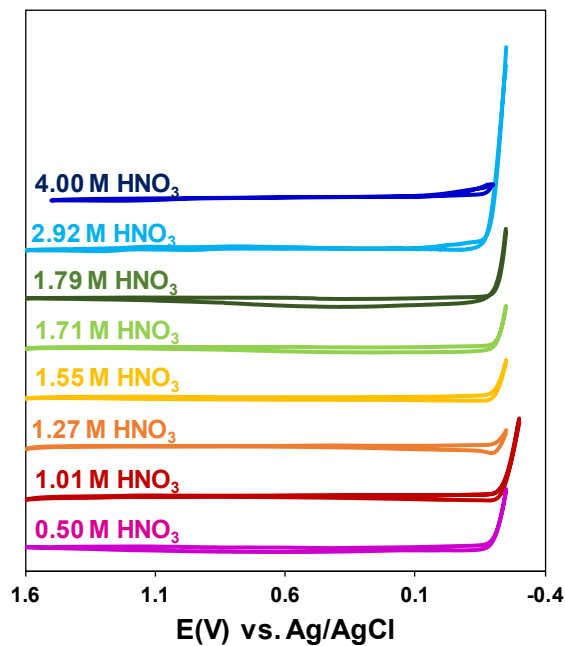


Figure S28. Cyclic voltammograms of HNO_3 in the absence of Np ($v = 100 \text{ mV s}^{-1}$): (bottommost purple trace) 0.50 M HNO_3 , (red trace second from bottom) 1.01 M HNO_3 , (orange trace third from bottom) 1.28 M HNO_3 , (yellow trace fourth from bottom) 1.55 M HNO_3 , (light green trace fourth from top) 1.71 M HNO_3 , (dark green trace third from top) 1.79 M HNO_3 , (light blue trace second from top) 2.92 M HNO_3 , (topmost dark blue trace) 4.00 M HNO_3 .

References:

- (1) Schroll, C. A.; Chatterjee, S.; Heineman, W. R.; Bryan, S. A. *Anal Chem* **2011**, *83*, 4214.
- (2) Konopka, S. J.; Mcduffie, B. *Anal Chem* **1970**, *42*, 1741.
- (3) Kim, S. Y.; Asakura, T.; Morita, Y. *Radiochim Acta* **2005**, *93*, 767.